Optimised photonic crystal waveguide for chiral light–matter interactions

You may also be interested in:

Dispersion engineered slow light in photonic crystals: a comparison
S A Schulz, L O'Faolain, D M Beggs et al.

Control of delay-bandwidth product in slow-light photonic crystal waveguides with asymmetric
microfluidic infiltration
M Jahanbakhshian and R Karimzadeh

Dispersion properties of photonic crystal waveguides with a low in-plane index contrast
M Augustin, R Iliew, C Etrich et al.

Photonic crystals waveguides based on wide-gap semiconductor alloys
Aude Martin, Sylvain Combrié and Alfredo De Rossi

Slow light modes for optical delay lines: 2D photonic crystal-based design structures,performances
and challenges
A Talneau

Slow-light Mach-Zehnder modulators based on Si photonic crystals
Toshihiko Baba, Hong C Nguyen, Naoya Yazawa et al.

Manipulating light with strongly modulated photonic crystals
Masaya Notomi

Group velocity enhancement for guided lightwave by band-pulling effect in single-mode silicon comb
photonic crystal wires
Borriboon Thubthimthong and Kazuhiro Hane

Optimised photonic crystal waveguide for chiral light–matter interactions

Ben Lang[1], Ruth Oulton[1] and Daryl M Beggs[2]

[1] Quantum Engineering Technology Labs, H. H. Wills Physics Laboratory and Department of Electrical & Electronic Engineering, University of Bristol, BS8 1FD, United Kingdom
[2] School of Physics and Astronomy, Cardiff University, Queen's Buildings, The Parade, Cardiff CF24 3AA, United Kingdom

E-mail: bl9453@bristol.ac.uk

CrossMark

Abstract
We present slow-light photonic crystal waveguide designs that provide a $\times 8.6$ improvement of the local density of optical states at a fully chiral point over previous designs.

Keywords: polarisation singularities, photonic crystal waveguides, slow light

(Some figures may appear in colour only in the online journal)

1. Introduction

Chirality of light in (nano-)photonic structures is proving to be a valuable resource [1–3]. In quantum optics, chirality couples the spin direction of electrons to the travel direction of light. This chiral light–matter interaction is at its most useful when the chirality reaches 100% at a singular position known as a C-point. A quantum dot (QD) placed at a C-point can display a spin-dependent unidirectional-emission [4] an attractive property for quantum optics, as it allows spin-encoded static qubits to be converted to path-encoded flying qubits. Further, ensembles of emitters coupled to a chiral waveguide can show remarkable entanglement properties [5, 6].

Photonic crystal waveguides (PhCWGs) present several unique benefits to realising chirality-direction coupling. Firstly, the longitudinal component of the waveguide modes is large, meaning that C-points with 100% chirality are common, and moreover tend to occur in the high-index part of the waveguide, where a QD could be placed. Secondly PhCWGs support slow-light. Extending the benefits of slow-light to the interaction of a QD at a C-point is attractive. Slow-light enhances the density of optical states allowing extremely bright sources and high collection efficiencies to be

realised [7]. In principle, there is no upper limit to the light–matter interaction enhancement. At the bandedge, the PhCWG has stopped modes with group velocity $v_g = 0$ and an infinite density of optical states (the van Hove singularity [8]). Only the practicality of fabricating a perfect waveguide without defects prevents the use of these bandedge modes.

As shown by our recent work, the case of an emitter placed at a C-point requires additional consideration. Time-reversal symmetry dictates that all chiral components of the waveguide mode must vanish in the stopped light at the bandedge, and therefore no C-points can be supported. Modes in the slow-light regime resemble the bandedge mode, and thus contain less chirality. This forces a compromise between strong light–matter interactions (for which slow light is desirable, typically found near the bandedge) and making those interactions chiral (for which we want powerful circularly polarised fields, which become scarce near the bandedge). We found that the optimum local density of optical states (LDOS) at a C-point is found in modes with modest group velocities of $v_g < c/10$ for the standard PhCWG design (the so-called W1 waveguide) [9]. Only a limited number of alternative nano-photonic designs for QDs have so-far been considered [10, 11]. In this paper we present alternative PhCWG designs that possess larger LDOS at the C-points.

Our search for these designs begins with the archetypal W1 waveguide of one row of missing holes from an hexagonal lattice of holes with radius $r = 0.3a$ in a GaAs dielectric membrane. We form new designs by displacing each
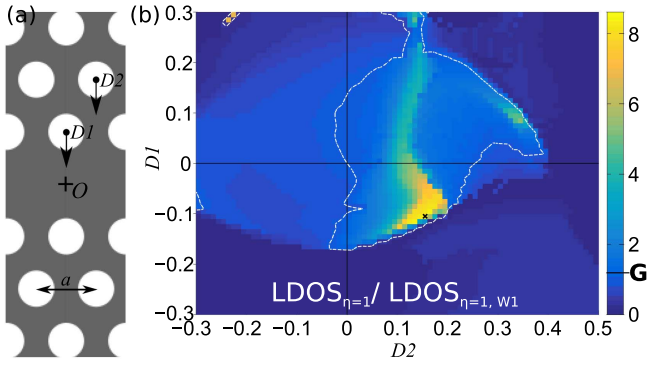
Figure 1. (a) The refractive index profile of a W1. The arrows indicate how $D1$ and $D2$ control the displacements of the innermost holes. O marks the origin of the in-plane coordinate system $(x, y) = (0, 0)$. (b) Largest LDOS at a C-point as a function of $(D1, D2)$, normalised to the largest LDOS at a C-point in a W1. The dotted line is a contour along which this ratio is unity. G on the colour bar indicates the value for the glide waveguide described in [10].

Figure 2. (a) 2d FDTD simulations of circular dipoles at the ideal points in the optimised and W1 waveguides. (b) Power radiated forwards, backwards and sideways: note the log scale.

hole in the first row of holes closest to the waveguide a distance $D1$ towards the waveguide core, and the second row of holes a distance $D2$ (figure 1(a)). In this way the dispersion [12] and electric field profile [13] of the PhCWG can be modified. Modifying the hole positions is preferred to the radii as they are more accurately realised in electron-beam lithography [14].

The LDOS is a function of position and frequency and is proportional to the product $n_g|E|^2$, where $n_g = |c/v_g|$ is the group index and $|E|^2$ is the electric field intensity. We are interested in positions of unit directionality, where the directionality is defined as the difference between power emitted by a spin transition (modelled as a circular point-dipole) into the forwards and backwards waveguide modes, normalised by the total power emitted into the waveguide. For a single-mode waveguide the directionality is simply given by the degree of chirality $\eta = |S_3| = 2|\mathrm{Im}(E_x^* E_y)|/|E|^2$. $\eta = 1$ is typically not possible if the waveguide is multi-mode (it requires the extraordinary coincidence of C-points at the same position in all modes at the same frequency) and so multi-mode frequency regions are ignored.

For each choice of $(D1, D2)$ we search for C-points with $\eta = 1$, and calculate the relative LDOS ($n_g|E|^2$) at each using a frequency domain eigensolver [16]. In each design $(D1, D2)$, the C-point with the highest LDOS is compared to the C-point with the highest LDOS in the W1 design $(D1, D2) = (0, 0)$. Our calculations use the effective index method [17], with $n_{\mathrm{eff}} = 2.66$, suitable for wavelengths around 900 nm and a GaAs membrane of thickness 100 nm. This 2d approximation shows good agreement with experiment over a wide range of circumstances [18, 19], although it has drawbacks: notably it tends to underestimate the group index near the bandedge [20] and naturally as a 2d method it misses 3d effects [21].

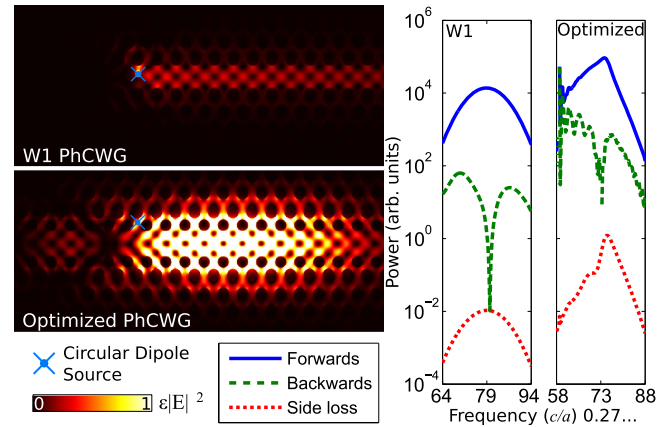We treat values of $n_g > 100$ as 100 in the LDOS calculation, serving the dual purpose of focusing the search on experimentally achievable values [22] and filtering computational errors at the bandedge where $|E|^2 \to 0$ and $n_g \to \infty$.

Figure 1(b) presents the main results, showing the enhancement of the LDOS at C-points where they occur in a single-mode waveguide. The vast majority of designs show little or no enhancement over the standard W1 (i.e. the ratio of LDOS at the C-points is below or close to one), but there is a small region of the search space that show significant enhancements. Of these, the best design identified has 8.61 times the C-point LDOS of a W1 for $(D1, D2) = (-0.11, 0.15)a$ at a C-point at frequency $0.2791c/a$ and position $(x, y) = (0.5, 1.170)a$ from the origin shown in figure 1(a). We repeated the calculations in 3d for a small subset of the best designs, and found good agreement with the 2d versions. However, a small shift of the optimal point was seen, to $(D1, D2) = (-0.07, 0.14)a$.

Finite difference time domain simulations confirming the unidirectional emission from the best identified C-points in the optimised and W1 waveguides are shown in figure 2(a) [15]. Our simulations are again 2d, using the same effective index approximation as above. Figure 2(b) shows the calculated power radiated in the forwards, backwards and sideways directions. The $\sim \times 10$ enhancement in LDOS is well replicated in these calculations. Emission into the backwards direction is suppressed by a factor of 10^6 in the W1 and 10^4 in the optimised design. In principle, emission in the backwards direction should be precisely zero for the correct location, polarisation and frequency of the dipole. However, away from this precise frequency, as the modes polarisation profile changes, the former C-point becomes elliptical and allows emission into the backwards direction. When the light is slower i.e. a smaller group velocity $v_g = \mathrm{d}\omega/\mathrm{d}k$ the change of wavevector and therefore mode profile is larger for a small change of frequency. Therefore slower light designs, such as the optimised waveguide, are likely to display a smaller bandwidth for high directionality and therefore the dip is not as well resolved in the simulation.

For these source locations in these waveguides the suppression of the backwards emission is over 100:1 for bandwidths of $\sim 2 \times 10^{-3}$ c/a and $\sim 4 \times 10^{-4}$ c/a. Even in the

latter case (the optimised waveguide) this is considerably larger than the linewidth of a QD (20 μeV $\sim 4 \times 10^{-6}$ c/a).

The best designs presented here exploit slow light far from the bandedge by flattening the dispersion. There is an element of brinkmanship to this, as flattening the dispersion towards an inflection-like curve maximises the LDOS, but overshooting creates a multimode region that ruins the performance. This abrupt drop is visible in figure 1(b) on the lower side of the bright region.

This motivates a minor digression. In principle a perfect inflection point in the dispersion appears able to support uni-directionality with an infinite density of states. However even infinitesimal perturbations (for example, from disorder) can break the inflection point into a local maximum and local minimum pair with a small separation. This local maximum/minimum pair results in a multi-mode region with a slow-light mode allowing (strong) emission in both directions. Although such abruptness may at first glance seem un-physical, it is a consequence of us considering only modes with real k_x (propagating modes), equivalent to considering an infinitely long PhCWG. Evanescent modes in a finite PhCWG always allow some light to tunnel from the dipole out of the waveguide in the wrong direction. Near an inflection point there exist weakly evanescent modes (with small imaginary k_x) that can tunnel a long distance [23]. These weakly evanescent modes smooth out this transition in finite-length PhCWGs.

In real-world samples, QDs are typically strain-grown in random locations [24] (although positioning methods are being developed [25]). Furthermore, the size and shape dispersion means that the resonant frequencies of the QDs are randomly distributed around the desired one. Experiments then typically proceed by testing a large number of samples, until a suitable one is found.

In the above, we have calculated the performance of the PhCWG for an ideally placed QD pitched at the ideal frequency, but we are also interested in the yield: how many samples can we expect to test before finding a good QD positioned at or near a C-point. To answer this question we have also calculated the probability that a QD placed at a random location in the GaAs with a random frequency (selected uniformly from the bandwidth of the fundamental mode) will have $\eta > 0.9$. Our calculations neglect positions with negligible LDOS and assume $\eta < 0.9$ at multimode frequencies.

Figure 3 shows the result of this calculation. The optimised waveguide identified above (white cross, figrue 3) has a poor yield ($\sim$1%). However by consideration of figures 1(b) and 3 together PhCWGs with a desired compromise of yield and performance can be chosen. For example for $(D1, D2) = (0.13, 0.13)$ the yield is 33% (for a W1 the yield is 24%) and the maximum LDOS is 4$\times$ greater than that in a W1. Nearby values offer a different trade-off between yield and LDOS enhancement.

In conclusion we have identified modified PhCWG designs that promise significant increases in chiral performance, with a $\times$8.6 enhancement of the LDOS. As the LDOS is a measure of the light–matter interaction strength, and is
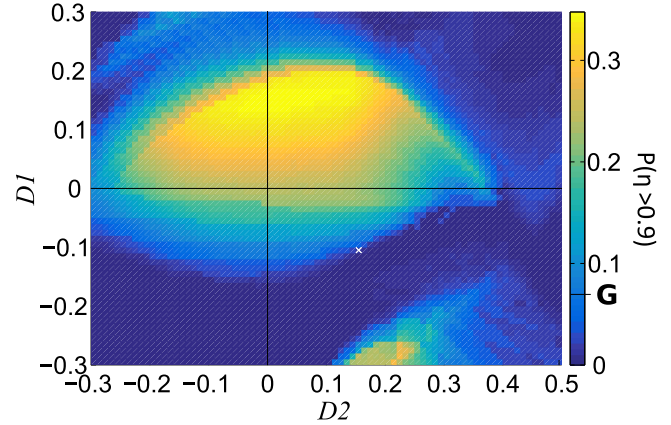
directly proportional to the emission rate and efficiency [16], our optimised design will allow fabrication of waveguides almost one order of magnitude brighter than using the standard W1 design.

In the final stages of this work we became aware of related work suggesting a modified glide-plane waveguide design for strong chiral interactions [26]. Our calculations suggest this design is excellent with >100 times LDOS enhancement at the best C-point compared to a W1 (see figure 1) and a $\sim$15% yield (see figure 3).

Figure 3. Calculated yield. The probability that directionality η exceeds 0.9 for randomly placed QDs. G has the same meaning as in figure 3.

Acknowledgments

References

[1] Lodahl P, Mahmoodian S, Stobbe S, Rauschenbeutel A, Schneeweiss P, Volz J, Pichler H and Zoller P 2017 Chiral quantum optics *Nature* **541** 473–80
[2] Rodríguez-Fortuño F J, Puerto D, Griol A, Bellieres L, Martí J and Martínez A 2014 Universal method for the synthesis of arbitrary polarization states radiated by a nanoantenna *Laser Photonics Rev.* **8** 3
[3] Neugebauer M, Bauer T, Banzer P and Gerd L 2014 Polarization tailored light driven Directional optical nanobeacon *Nano Lett.* **14** 5
[4] Young A B, Thijssen A C T, Beggs D M, Androvitsaneas P, Kuipers L, Rarity J G, Hughes S and Oulton R 2015

Polarization engineering in photonic crystal waveguides for spin-photon entanglers *Phys. Rev. Lett.* **115** 153901

[5] Mirza I M and Schotland J C 2016 Multiqubit entanglement in bidirectional-chiral-waveguide QED *Phys. Rev.* A **94** 012302

[6] Ramos T, Pichler H, Daley A J and Zoller P 2014 Quantum spin dimers from chiral dissipation in cold-atom chains *Phys. Rev. Lett.* **113** 237203

[7] Arcari M *et al* 2014 Near-unity coupling efficiency of a quantum emitter to a photonic crystal waveguide *Phys. Rev. Lett.* **113** 093603

[8] Van Hove L 1953 The occurrence of singularities in the elastic frequency distribution of a crystal *Phys. Rev. Lett.* **89** 1189

[9] Lang B, Beggs D M and Oulton R 2016 Time-reversal constraint limits unidirectional photon emission in slow-light photonic crystals *Phil. Trans. R. Soc.* A **374** 2075

[10] Söllner I *et al* 2015 Deterministic photon-emitter coupling in chiral photonic circuits *Nat. Nanotechnol.* **10** 775–8

[11] Coles R J, Price D M, Dixon J E, Royall B, Clarke E, Kok P, Skolnick M S, Fox A M and Makhonin M N 2016 Chirality of nanophotonic waveguide with embedded quantum emitter for unidirectional spin transfer *Nat. Commun.* **7** 11183

[12] Li J, White T P, O'Faolain L, Gomez-Iglesias A and Krauss T F 2008 Systematic design of flat band slow light in photonic crystal waveguides *Opt. Express* **16** 6227–32

[13] O'Faolain L *et al* 2010 Loss engineered slow light waveguides *Opt. Express* **18** 27627–38

[14] Schulz S A, O'Faolain L, Beggs D M, White T P, Melloni A and Krauss T F 2010 Dispersion engineered slow light in photonic crystals: a comparison *J. Opt.* **12** 104004

[15] Oskooi A F, Roundy D, Ibanescu M, Mihai P B, Joannopoulos J D and Johnson S G 2010 Meep: a flexible free-software package for electromagnetic simulations by the FDTD method *Comput. Phys. Commun.* **181** 687–702

[16] Johnson S G and Joannopoulos J D 2001 Block-iterative frequency-domain methods for Maxwell's equations in a planewave basis *Opt. Express* **8** 173–90

[17] Qiu M 2002 Efective index method for heterostructure-slab-waveguide-based two-dimensional photonic crystals *Appl. Phys. Lett.* **81** 7

[18] Corcoran B, Monat C, Grillet C, Moss D J, Eggleton B J, White T P, O'Faolain L and Krauss T F 2009 Green light emission in silicon through slow-light enhanced third-harmonic generation in photonic-crystal waveguides *Nat. Photon.* **3** 206–10

[19] Faggiani R *et al* 2016 Lower bound for the spatial extent of localized modes in photonic-crystal waveguides with small random imperfections *Sci. Rep.* **6** 27037

[20] Schulz S A, Park A H K, de Leon I, Upham J and Boyd R W 2015 Beyond the effective index method: improved accuracy for 2D simulations of photonic crystal waveguides *J. Opt.* **17** 075006

[21] Gansch R, Kalchmair S, Genevet P, Zederbauer T, Detz H, Andrews A M, Schrenk W, Capasso F, Lončar M and Strasser G 2016 Measurement of bound states in the continuum by a detector embedded in a photonic crystal *Light: Sci. Appl.* **5** e16147

[22] Vlasov Y A, O'Boyle M, Hamann H F and McNab S J 2005 Active control of slow light on a chip with photonic crystal waveguides *Nature* **438** 65–9

[23] White T P, Botten L C, Martijn de Sterke C, Dossou K B and McPhedran R C 2008 Efficient slow-light coupling in a photonic crystal waveguide without transition region *Opt. Lett.* **33** 2644–6

[24] Leonard D, Krishnamurthy M, Reaves C M, Denbaars S P and Petroff P M 1993 Direct formation of quantum-sized dots from uniform coherent islands of InGaAs on GaAs surfaces *Appl. Phys. Lett.* **63** 3203

[25] Schneider C, Strauß M, Sünner T, Huggenberger A, Wiener D, Reitzenstein S, Kamp M, Höfling S and Forchel A 2008 Lithographic alignment to site-controlled quantum dots for device integration *Appl. Phys. Lett.* **92** 183101

[26] Mahmoodian S, Prindal-Nielsen K, Söllner I, Stobbe S and Lodahl P 2017 Engineering chiral light–matter interaction in photonic crystal waveguides with slow light *Opt. Mater. Express* **7** 43–51